Dielectric and infrared properties of $SrTiO_3$ single crystal doped by 3d (V, Mn, Fe, Ni) and 4f (Nd, Sm, Er) ions*

S. Maletic[a)†], D. Maletic[b)], I. Petronijevic[a)], J. Dojcilovic[a)], and D. M. Popovic[a)]

[a)] *Faculty of Physics, University of Belgrade, Studentski trg* 12–14, 11000 *Belgrade, Serbia*
[b)] *Institute of Physics, University of Belgrade, Pregrevica* 118, 11080 *Belgrade, Serbia*

(Received 7 March 2013; revised manuscript received 9 July 2013; published online 10 December 2013)

In this study, the effects of doping by 3d (V, Mn, Fe, Ni) and 4f (Nd, Sm, Er) ions on dielectric and infrared properties of $SrTiO_3$ (STO) single crystals are investigated. It is well known that doping of the $SrTiO_3$ can change the dielectric properties of the STO from an insulator to an n-type semiconductor, and even to a metallic conductor. Dielectric and infrared (IR) properties of the undoped STO and doped STO single crystals are analyzed using dielectric spectroscopy (80 kHz–5 MHz), transmission (200 cm^{-1}–4000 cm^{-1}), and reflection spectroscopy (50 cm^{-1}–2000 cm^{-1}). It is found that doping by the 3d ions reduces the value of dielectric permittivity, but the trend of temperature dependence of the dielectric permittivity remains almost unchanged. On the other hand, dielectric spectroscopy measurements for samples doped by 4f ions show the anomalous behaviors of the dielectric permittivity at temperatures around the temperature of the structural phase transition. There are two fractures of temperature dependences of inverse dielectric permittivity $\varepsilon_r^{-1}(T)$. Transmittance spectroscopy measurements show that there are differences in the shape of the spectrum in the mid-IR region between the undoped STO and the one doped by 4f ions. The differences in the reflectance spectrum between the STO:Nd and STO are analyzed in detail.

Keywords: doping, dielectric properties, phase transitions, infrared spectroscopy

PACS: 61.72.S−, 63.20.−e, 77.22.Ch, 78.20.Ci **DOI:** 10.1088/1674-1056/23/2/026102

1. Introduction

Strontium titanate $SrTiO_3$ (STO) with its $3d^0$ electronic configuration is a wide band insulator. It was the first material in which the strong increase of static dielectric permittivity at low temperatures was demonstrated to be associated with the softening of a long-wavelength transverse optic phonon mode.[1]

The STO has been of particular importance from the perspective of fundamental solid state physics, as well as in technological applications. Because of its good dielectric properties, it has become very usable in devices in integrated microelectronics and in memory storage.[2–4] Also, the $SrTiO_3$ has gained additional practical importance as the most widely used substrate for depositing high–T_c superconducting films.[5–7] As experiments on semitransparent samples are becoming more common, it is important to know the substrate dielectric function in order to correctly analyze the optical measurements performed on film plus the substrate system.[8,9]

Doping is often used to change the dielectric properties of the STO.[10–12] It has been well documented that a small number of impurity ions can change the properties of this interesting system.[13–15] Doped $SrTiO_3$ is widely used in the industry in order to manufacture voltage-dependent resistors and as a transparent electrode.[3]

Also, the electrical properties of strontium titanate strongly depend on its oxygen content.[16,17] The removal of oxygen from a lattice site acts as a dopant because the two electrons of the O^{2-} ions are left in the crystal and oxygen escapes as a neutral atom in order to maintain charge neutrality. Therefore, creating an oxygen vacancy in the STO is considered as an n-type doping.[18] Electron doping to the STO by oxygen vacancies or the substitution of cations with different valences can generate many intriguing physical properties, such as superconductivity, nonvolatile resisting switching, and a metallic state with extremely low carrier density.[2,19–21]

In order to understand these properties of the doped STO, the study of changes in the dielectric properties that arise as a result of the incorporation of different cations is essential. In the present research, the influence of doping by the 3d- (Mn, V, Fe, Ni) and 4f- (Nd, Sm, Er) ions on the dielectric and infrared (IR) properties of the STO single crystal are examined by using dielectric measurements in a temperature range of 30 K–300 K and a frequency range of 80 kHz–5 MHz, and also by using the transmission infrared spectroscopy in a range of 200 cm^{-1}–4000 cm^{-1} and the reflection measurements in a range of 50 cm^{-1}–2000 cm^{-1}.

2. Material and method

The investigated single crystal samples for these experiments were grown by using the Verneuil technique.[22] The concentrations of 3d-ions (V, Mn, Fe, Ni) are all 5×10^{-2} at.% and the concentrations of 4f-ions i.e., ions of rare earth (RE),

*Project supported by the Science Fund from the Ministry of Education and Science of the Republic of Serbia (Grant No. 171029).
†Corresponding author. E-mail: sslavica@ff.bg.ac.rs
© 2014 Chinese Physical Society and IOP Publishing Ltd

Nd, Sm, Er are all 2×10^{-3} at.%.

The samples were obtained as small plates with thickness values of $l = 0.8$ mm–1 mm, each with a diameter (d) of about 10 mm; that is, $d \approx 10$ mm. The colors of the STO samples doped by Nd, Sm, and Er are found to be dark gray, in contrast to the transparency of the pure STO.

The dielectric measurements of the pure and doped $SrTiO_3$ single crystals were performed in a frequency range from 80 kHz to 5 MHz using a computer-controlled Agilent Precision LCR Meter 4285A. The samples in the form of plate were placed in a stainless steel cell with an AC signal of 1.5 V applied across the cell. The control of the sample temperature in a range of 30 K–300 K was achieved by using the CTI-Cryogenics Cryodyne closed loop system and the Lake Shore 340 temperature controller.[23]

The transmission spectra were scanned in a frequency range of 200 cm^{-1}–4000 cm^{-1} using the Perkin Elmer 883 spectrometer at room temperature.

The reflectivity spectra were measured with a BOMEM DA-8 spectrometer. The disc-shaped pellets were optically polished by using a diamond paste. The sizes of the diamond grains were less than 1 μm. A deuterated triglycine sulfate (DTGS) pyro-electric detector was used to cover the wave-number range from 50 cm^{-1} to 600 cm^{-1} and a liquid-nitrogen-cooled Hg–Cd–Te detector was used in a wave-number range from 500 cm^{-1} to 5000 cm^{-1}. The spectra were collected with a 2-cm^{-1} resolution. For low-temperature measurements, a Janis Super Tran (ST-100) continuous flow cryostat was used. For the reference mirror, an evaporated Au film was used.

3. Results and discussion

3.1. Dielectric measurements

The strontium titanate is known as a quantum paraelectric.[11,24] The temperature dependence of the dielectric permittivity at temperatures below room temperature and above 50 K can be described by the Curie–Weiss law $\varepsilon_r = C/(T-\theta)$.[24–26] At low temperatures ($T < 50$ K), the permittivity deviates from this law, and the temperature dependence of the dielectric permittivity can be described by the Barrett's formula.[27] This deviation is explained by the existence of quantum fluctuations that prevent long-range ordering.

In previous papers[28,29] we analyzed $\varepsilon_r(T)$ dependences for the test frequency 1 MHz. In an attempt to reach additional information about the STO doped by the 3d and 4f ions, we investigated $\varepsilon_r(T)$ dependences for a frequency range of 80 kHz–5 MHz. Some of the most important results are presented in this paper.

Figure 1 shows the plots of dielectric permittivity as a function of the temperature and frequency for the undoped

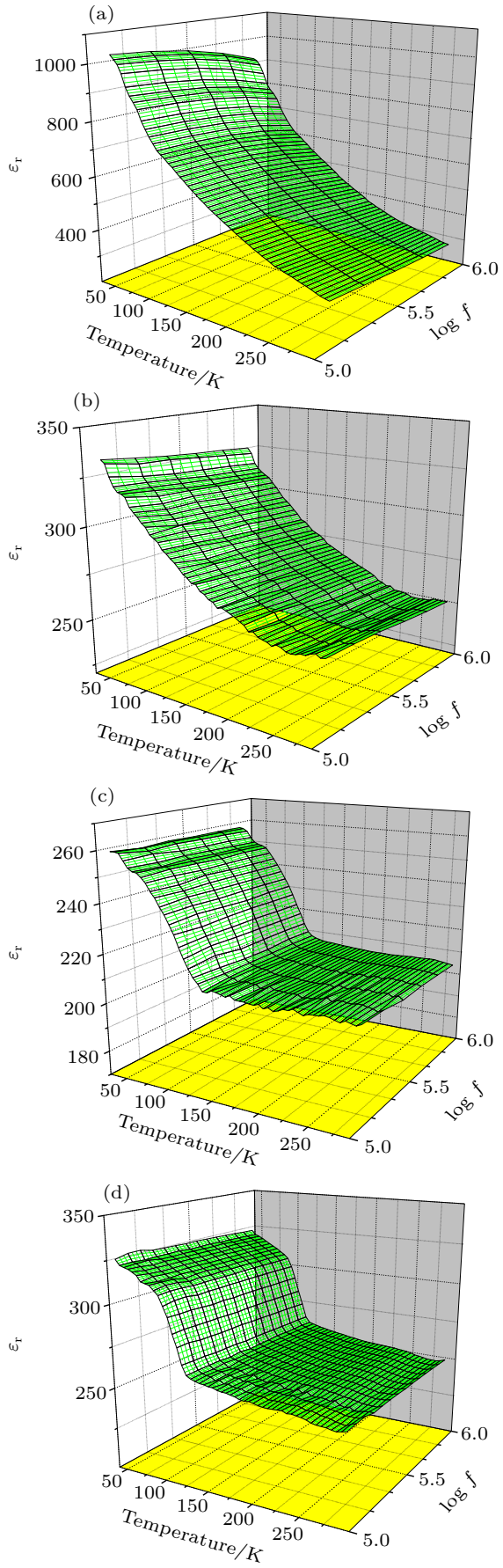


Fig. 1. (color online) Plots of dielectric permittivity versus temperature and logarithm of frequency for (a) $SrTiO_3$, (b) $SrTiO_3$:Ni, (c) $SrTiO_3$:Nd, and (d) $SrTiO_3$:Sm single crystals.

STO and the doped STO:Ni, STO:Nd, STO:Sm single crystals, respectively. For all the investigated samples, the values of the dielectric permittivity decrease with an increase in temperature for all the test frequencies and they generally follow a Curie–Weiss law. Also, it is visible that the temperature dependence of the dielectric permittivity is poorly dependent on test frequency. Furthermore, doping the STO by Ni ions has no effect on the trend of temperature dependence of the dielectric permittivity of the $SrTiO_3$. A similar temperature dependence of the dielectric permittivity has been obtained for other investigated samples doped by the 3d ions and some of them have previously been reported.[28–30] The values of the dielectric permittivity for all the investigated samples which are doped by the 3d-ions are lower than the corresponding values of the undoped STO crystal.

Our measurements of $\varepsilon_r(T)$ for the undoped STO confirmed the well-known literature fact that the existence of the antiferrodistortive structural phase transition at temperature 105 K does not lead to anomalies in the dependence of $\varepsilon_r(T)$.[24,25]

In contrast to the dependences in Figs. 1(a) and 1(b), figures 1(c) and 1(d) show that there are changes in the growth rate of the dielectric permittivity for the temperatures below 120 K for samples doped by the 4f (Nd and Sm) ions.

In order to facilitate the comparison, the inverse dielectric permittivity for the sample STO:Nd (the test frequency of 0.1 MHz) is presented in Fig. 2. The two fractures could be clearly noticed at $\varepsilon_r^{-1}(T)$ dependence at temperatures $T_1 =$ 77 K and $T_2 = 120$ K, and the well-known structural phase transition belongs to the interval 77 K–120 K. From the inset of Fig. 2, one can notice the existence of a slight fracture of the $\varepsilon_r^{-1}(T)$ dependences for STO:Ni.

The difference between the noticeable transition of the STO:Ni and the clearly visible transition of the STO doped by the 4f ions may indicate a significant difference between the roles which 3d and 4f ions played in the host lattice. Also, in Fig. 2 one can see that, from the standpoint of the structural phase transition, the undoped STO and the STO doped by the 3d are similar to each other, while the STO doped by the 4f ions differs from them significantly. In other words, while the doping by 3d ions slightly changes the ε_r around the temperature of the structural phase transition, doping by the 4f ions has a drastic influence.

In an attempt to enlighten the origins of these differences, we analyze the role of the partial tolerance factor in detail. The degree of the packing of A or B ions in the perovskite lattice ABO_3 is well described by the fractional tolerance factors $t_1 = \sqrt{2}(r_A + r_O)/a$ and $t_2 = 2(r_B + r_O)/a$, where a is the lattice parameter and r_A, r_B, and r_O are radii of the corresponding ions.[31,32] The lattice parameter of the undoped samples has a value of 0.3905 nm.[33] When t_1 or $t_2 < 1$ the A or B ions fluctuate at their sites, whereas when t_1 or $t_2 > 1$ the A or B ions are closely packed.[31]

Table 1 shows the estimated partial tolerance factors for 3d (V, Mn, Fe, Ni) and 4f (Nd, Sm, Er) ions. The 3d elements with the coordination number 6 have ionic radii similar to the radius of Ti ion. The radius of the Ti^{4+} in the 6-fold octahedral coordination is 0.605 Å (1 Å = 0.1 nm).[34] Because of this, we suppose that 3d-ions preferably occupy B positions. For these ions, the calculated values of the fractional tolerance factor t_2 are greater than 1 (see Table 1). According to this, 3d-ions are closely packed in the $SrTiO_3$ lattice.

Table 1. Values of partial tolerance factors t_1 and t_2 for 3d and 4f ions in STO.

Ion	Coordination number	Valence	Ionic radius/Å	Partial tolerance factor t_2	Partial tolerance factor t_1
Ti	VI	3+	0.67	1.06	
Ti	VI	4+	0.605	1.027	
V	VI	2+	0.79	1.121	
V	VI	4+	0.58	1.014	
Mn	VI	2+	0.67	1.060	
Fe	VI	2+	0.83	1.142	
Ni	VI	4+	0.53	0.99	
Ni	VI	2+	0.69	1.070	
Nd	VI	3+	0.98	1.220	
Sm	VI	3+	1.03	1.244	
Er	VI	3+	0.89	1.172	
Sr	XII	2+	1.44		1.025
Nd	XII	3+	1.27		0.967
Sm	XII	3+	1.24		0.956
Er	XII	3+	1.15		0.923

The valence of rare earth ions in the perovskite oxides is usually 3+.[35,36] The ionic radii of 4f-ions Sm^{3+}, Nd^{3+}, Er^{3+} are close to the radius of Sr^{2+} ion. The radius of Sr^{2+} in the 12-fold dodecahedral coordination is 1.44 Å. This indicates that the RE^{3+} ions could preferably occupy the A site in perovskite lattice. In that case, the RE^{3+} acts as a donor dopant and the local charge compensation is needed. The produced electrons can be trapped by the Ti^{4+} ions with respect to the formation of the Ti^{3+}. From Table 1, one can see that the values of the corresponding partial tolerance factor t_1 for RE^{3+} ions are all lower than 1. This indicates that these ions could fluctuate at the A-site, which could lead to the conclusion that they are not as tightly packed in the crystal lattice as the 3d ions. Furthermore, the introduction of the rare-earth ions into the STO crystal lattice causes the interionic RE–O distance to be different from that of the Sr–O ones, therefore, leading to the changes in the polarizability of the ions while also compromising the regular shape of the TiO_6 octahedron. On the other hand, the TiO_6 octahedron plays a crucial role in the structural phase transition ($T = 105$ K). The lack of fracture in the temperature dependence of the dielectric permittivity for the 3d-doped samples (Fig. 2) could indicate that the 3d doping has no significant influence on a network composed of TiO_6 octahedra.

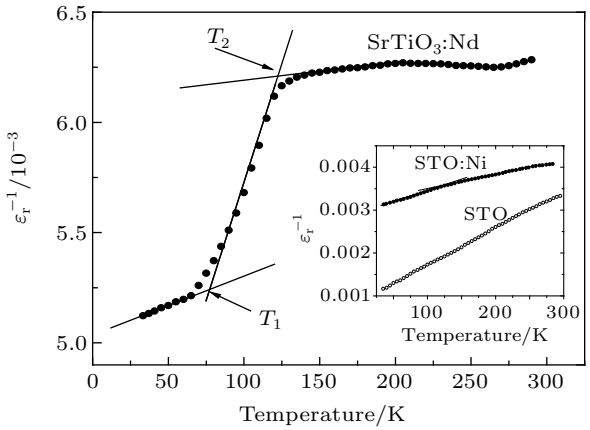


Fig. 2. Inverse dielectric permittivity versus temperature of STO:Nd at test frequency 0.1 MHz. Temperatures T_1 and T_2 indicate the crossover between three different regimes. The known structural phase transition belongs to intervals T_1–T_2. Inset shows the plots of inverse dielectric permittivity versus temperature of doped STO:Ni and undoped STO.

3.2. Transmission spectra

Figures 3 and 4 present the transmission spectra of the undoped STO and the doped STO in a range of 200 cm^{-1} –4000 cm^{-1} at room temperature. Figures 3(a)–3(d) show transmission spectra of the undoped STO and the STO doped by 3d ions (V, Mn, Fe, Ni), respectively. One can see that the undoped $SrTiO_3$ is transparent above 1350 cm^{-1}, which is consistent with the results published by Dore *et al.*[9] The shapes of the spectrum of the doped samples are very similar to the shape of a spectrum of the undoped STO. The absorption values are large in a range of 200 cm^{-1}–1350 cm^{-1} for all investigated samples.

The transmission spectra of the undoped STO and the 4f ions (Nd, Sm, and Er) doped STO are shown in Figs. 4(a)–4(c), respectively. The obtained spectra show that the transmissions are very low (below 5%) in a range of 200 cm^{-1}–4000 cm^{-1} for all the investigated samples doped by rear earth ions.

Generally, the far-IR absorption of the $SrTiO_3$ is attributed to the lattice absorption and the free-carrier absorption. The large absorption in a range of 1350 cm^{-1}–4000 cm^{-1} could be explained by various theories taking into account differences in electronic structure, electron-lattice coupling, oxygen clustering or defects, between 3d and 4f ions in the crystal lattice.[37–39]

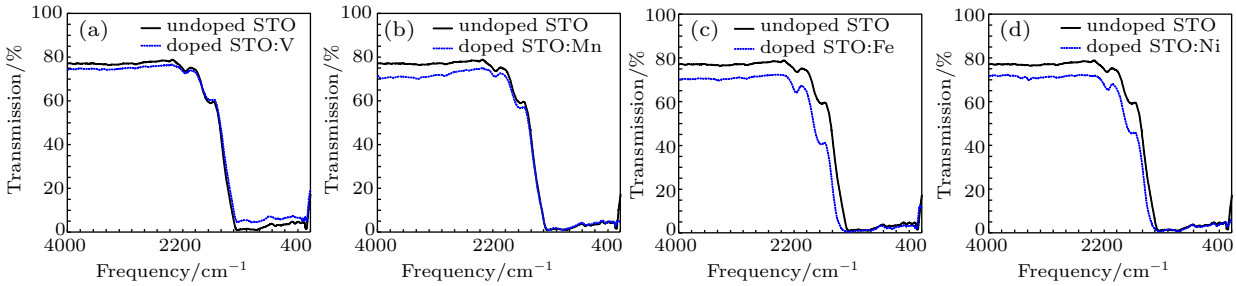


Fig. 3. (color online) Transmission spectra of the undoped STO single crystal and 3d ions doped (a) STO:V, (b) STO:Mn, (c) STO:Fe, (d) STO:Ni.

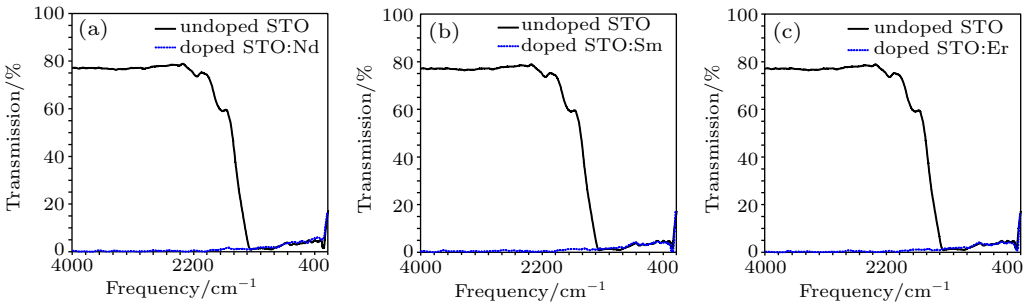


Fig. 4. (color online) Transmission spectra of the undoped STO single crystal and 4f ions doped (a) STO:Nd, (b) STO:Sm, (c) STO:Er.

3.3. Reflectance measurements

Figure 5 shows the reflectance spectra of the pure $SrTiO_3$ single crystals in a frequency range of 50 cm^{-1}–1200 cm^{-1} at temperatures $T = 300$ K and $T = 80$ K. There are three broad bands in both spectra, which is in good accordance with the data in the literature.[8,14] The first one of these bands (TO_1–LO_1) is located below 160 cm^{-1}, the second one (TO_2–LO_2) is in a range from 170 cm^{-1} to 500 cm^{-1}, and the third one (TO_3–LO_3) from 550 cm^{-1} to 800 cm^{-1}. It is well known that a low-frequency band decreases with temperature decreasing, which is typical behavior for the soft mode above the phase transition temperature.[40] Also, the extraordinarily large intensity of the lowest phonon energy is responsible for high dielectric constant behavior.[8,30]

In order to enlighten the influence of the 4f ions on the di-

electric properties of the STO single crystal, we analyzed the reflectance spectra of the $SrTiO_3$:Nd in detail.

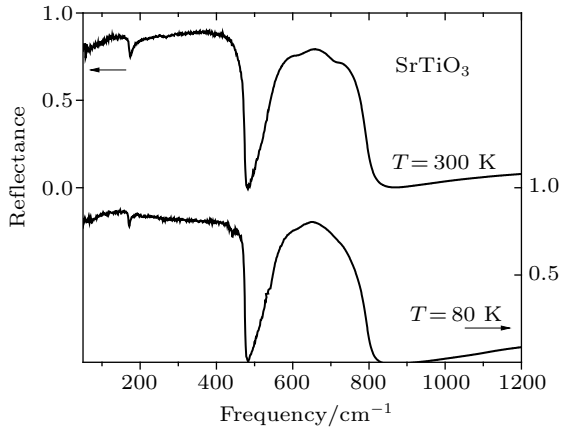


Fig. 5. Reflectance spectra of $SrTiO_3$ single crystal at $T = 300$ K and $T = 80$ K.

Figure 6 shows the reflectance spectra of the STO and the STO:Nd single crystal in a wave number range of 50 cm^{-1}–4000 cm^{-1} at $T = 300$ K. The shapes of the spectra of the doped samples are very similar to the one of the undoped STO for the frequencies above 400 cm^{-1}. Absolute values of the IR reflectivity are much lower for the Nd-doped crystal than for the pure one. These values are presumably lower due to the presence of surface imperfections of the crystal.

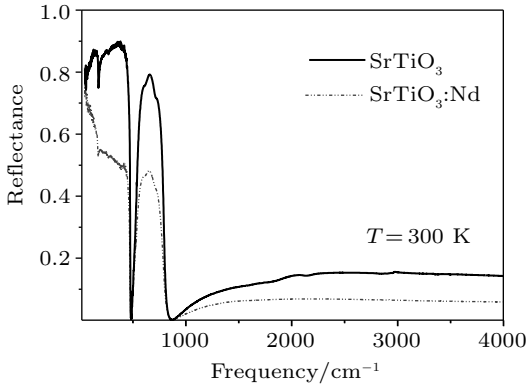


Fig. 6. Reflectance spectra of undoped $SrTiO_3$ and doped $SrTiO_3$:Nd single crystals at temperature $T = 300$ K.

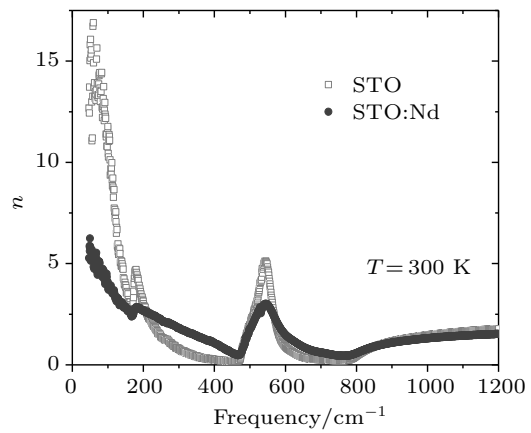


Fig. 7. Plots of real part of the complex index of refraction n versus frequency for STO and STO:Nd single crystals, determined using a KK-analysis.

The Kramers–Kronig (KK) transformations of $R(\omega)$ are performed. The standard high-frequency and low frequency extrapolation were used.[8] Figure 7 shows the plots of real part of the complex index of refraction $n(\sqrt{\tilde{\varepsilon}} = \tilde{n} = n + ik)$ versus frequency, obtained from KK-analysis of the reflectivity at a temperature of 300 K for the STO and STO:Nd.

Figures 6 and 7 show that doping by the Nd ions causes the differences at frequencies below 200 cm^{-1} for $R(\omega)$ and, consequently, the $n(\omega)$ spectra. In other words, the Nd-doping significantly affects the lowest frequency phonon mode.

Based on the band structure calculations of the STO[20,41] the top of the valence band is composed of the oxygen 2p states, and the bottom of the unoccupied conduction band presents the Ti 3d t_{2g} characteristics. The existence of the energy gap between the O 2p state and the Ti 3d state causes the insulating characteristic of the $SrTiO_3$ and the network of corner-sharing TiO_6 octahedra determines the main electronic properties of the STO. When the RE^{3+} ions are introduced into the compound, the transition from Ti^{4+} to Ti^{3+} takes place through an electronic compensation mechanism; thus, an empty d-orbital is partially filled with electrons. Therefore, we assume that this influence is primarily achieved by changing the density of the free charge carries.

Both $R(\omega)$ spectra are fitted by well-known Fresnel formula.[42] In the case of pure STO, the factorized form of the complex dielectric function Eq. (1) is used[8]

$$\varepsilon(\omega) = \left[\varepsilon_\infty \prod_{j=1}^{3} \frac{\omega_{\mathrm{LO}_j}^2 - \omega^2 + \mathrm{i}\gamma_{\mathrm{LO}_j}\omega}{\omega_{\mathrm{TO}_j}^2 - \omega^2 + \mathrm{i}\gamma_{\mathrm{TO}_j}\omega}\right], \tag{1}$$

where ω_{LO_j}, ω_{TO_j}, γ_{LO_j}, and γ_{TO_j} are frequencies and damping of j-th LO and TO modes, respectively; ε_∞ is the dielectric constant at high frequencies. For the initial values of the parameters in the fitting process, we take the values reported by Kamaras *et al.*[8] In order to test the assumption regarding the roles of the free charge carriers in the $R(\omega)$ spectra, for the STO:Nd we use the modified fitting function, which is achieved by adding the Drude contribution

$$\left[-\frac{\omega_\mathrm{p}^2 - \mathrm{i}(\gamma - \gamma_0)\omega}{\omega(\omega + \mathrm{i}\gamma_0)}\right] \tag{2}$$

to the factorized form of the dielectric function, where ω_p is the plasma frequency, γ is the linewidth of the plasma response at $\omega = \omega_\mathrm{p}$, and γ_0 is the linewidth of the absorption centered at $\omega = 0$.

The corresponding best-fitting values of the observed spectra are given in Table 2. The Table 2 contains the results of a fitting procedure for the reflectance spectra of the single crystal STO:Mn which is used here as representatives of the STO doped by 3d ions, while the corresponding reflection spectra were presented elsewhere.[30] The reflectance spectrum of the STO:Mn is very similar to that of the undoped one, which is why we used a factorized model of the dielectric function (Eq. (1)).

Table 2. Values of parameters from the best fitting. (All values are in unit cm^{-1}).

	STO	STO:Nd	STO:Mn[30]
ω_{TO1}	91	87	93
ω_{LO1}	169	160	171
ω_{TO2}	173	175	174
ω_{LO2}	471	474	474
ω_{TO3}	548	544	545
ω_{LO3}	790	781	782
ω_p		198	

The results of the fitting procedure and experimental data for the STO and STO:Nd are shown in Fig. 8. One can see the agreement between the experimental data and the best fitting, which confirms the success of the used model. The lattice dynamic properties of these phonon modes and carrier concentrations should be studied in further investigations.

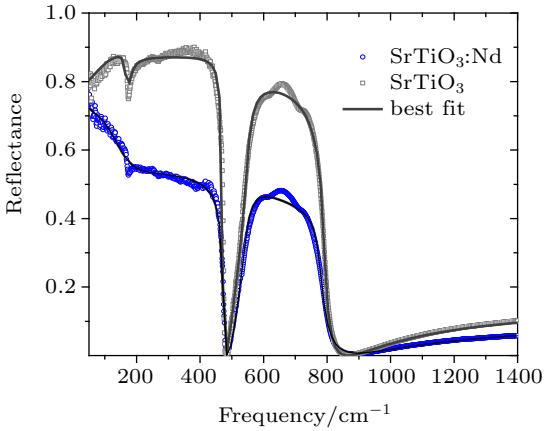


Fig. 8. (color online) Experimental and fitted reflectivity spectra of $SrTiO_3$ and $SrTiO_3$:Nd at 300 K. The experimental data are represented by symbols. The solid lines through the data are based on the calculations by using the best-fit parameters.

4. Conclusions

We studied the dielectric and infrared properties of the STO single crystals doped by 3d (V, Mn, Fe and Ni) and 4f (Sm, Nd and Er) ions. In general, doping by the 3d ions does not have a significant effect on the properties of the STO single crystal, both dielectric and spectral. Nevertheless, it has been found that, at the same temperature, the values of the dielectric permittivity of the samples doped by the 3d-ions are lower than those of the undoped STO samples for the whole frequency range.

In contrast, the doping with the 4f ions affects both the dielectric and spectral properties of the STO single crystals. We suppose that the influence of such doping is achieved in two ways. Firstly, by analyzing the T-dependence of the dielectric permittivity, keeping in mind that the STO is a highly polarizable crystal, we could suppose that the 4f-doping of the STO will significantly affect the mechanism of polarization. Secondly, the RE doping affects the impurity–lattice interaction and the increases of the density of charge carries density. By improving the four-parameter fitting function, we have clearly demonstrated the significance of the role which the free carriers play in STO:RE crystals.

References

[1] Viana R, Lunkenheimer P, Hemberger J, Böhmer R and Loidl A 1994 *Phys. Rev. B* **50** 601
[2] Waser R, Dittmann R, Staikov G and Szot K 2009 *Adv. Mater.* **21** 2632
[3] Gevorgian S 2009 *Ferroelectrics in Microwave Devices, Circuits and Systems* (London: Springer) p. 62
[4] Ma Z Z, Li J Q, Tian Z M, Qiu Y and Yuan S L 2012 *Chin. Phys. B* **21** 107503
[5] Shields T C, Abell J S, Button T W, Chakalov R A, Chakalova R I, Cai C, Haessler W, Eickemeyer J and de Boer B 2002 *Physica C* **372–376** 747
[6] Wang Q Y, Li Z, Zhang W H, Zhang Z C, Zhang J S, Li W, Ding H, Ou Y B, Deng P, Chang K, Wen J, Song C L, He K, Jia J F, Ji S H, Wang Y Y, Wang L L, Chen X, Ma X C and Xue Q K 2012 *Chin. Phys. Lett.* **29** 037402
[7] Gao J, Yang T, Ma P and Dai Y D 2010 *Chin. Phys. B* **19** 067402
[8] Kamarás K, Barth K L, Keilmann F, Henn R, Reedyk M, Thomsen C, Cardona M, Kircher J, Richards P L and Stehle J L 1995 *J. Appl. Phys.* **78** 1235
[9] Dore P, Paolone A and Trippetti R 1996 *J. Appl. Phys.* **80** 5270
[10] Bednorz J G and Müller K A 1984 *Phys. Rev. Lett.* **52** 2289
[11] Ang C, Yu Z, Hemberger J, Lunkenheimer P and Loidl A 1999 *Phys. Rev. B* **59** 6665
[12] Bianchi U, Kleemann W and Bednorz J G 1994 *J. Phys.: Condens. Matter* **6** 1229
[13] Ma J Y, Bi C Z, Fang X, Zhao H Y, Kamran M and Qiu X G 2007 *Physica C* **463–465** 107
[14] Gervais F, Servoin J L, Baratoff A, Bednorz J G and Binnig G 1993 *Phys. Rev. B* **47** 8187
[15] Yun J N, Zhang Z Y, Yan J F and Deng Z H 2010 *Chin. Phys. B* **19** 017101
[16] Jourdan M and Adrian H 2003 *Physica C* **388–389** 509
[17] Gentils A, Copie O, Herranz G, Fortuna F, Bibes M, Bouzehouane K, Jacquet É, Carrétéo C, Basletić M, Tafra E, Hamzić A and Barthéléy A 2010 *Phys. Rev. B* **81** 144109
[18] Gross H, Bansal N, Kim Y S and Oh S 2011 *J. Appl. Phys.* **110** 073704
[19] Schooley J F, Hosler W R and Cohen M L 1964 *Phys. Rev. Lett.* **12** 474
[20] Benthem K V, Elsässer C and French R H 2001 *J. Appl. Phys.* **90** 6156
[21] Yun J N, Zhang Z Y, Yan J F and Zhao W 2009 *Chin. Phys. Lett.* **26** 017107
[22] Byrappa K and Ohachi T 2003 *Crystal Growth Technology* (New York: William Andrew Inc., Norwich) p. 564
[23] Kulagin N, Dojcilovic J and Popovic D 2001 *Cryogenics* **41** 745
[24] Müller K A and Burkhard H 1979 *Phys. Rev. B* **19** 3593
[25] Weaver H E 1959 *J. Phys. Chem. Solids* **11** 274
[26] Marder M P 2000 *Condensed Matter Physics* (New York: Wiley-Interscience) p. 659
[27] Barrett J H 1952 *Phys. Rev.* **86** 118
[28] Kulagin N and Dojcilovic J 1999 *Physica B* **269** 49
[29] Dojcilovic J, Kulagin N, Popovic D and Spasovic S 2004 *Crystallography Reports* **49** 469
[30] Maletic S, Paunovic N, Popovic D and Dojcilovic J 2009 *Proceeding of the 7th International Conference of the Balkan Physical Union*, September 9–13, 2009, Alexandroupolis, Greece, p. 267
[31] Galasso F S 1969 *Structure, Properties and Preparation of Perovskite-Type Compounds* (Oxford: Pergamon) p. 3
[32] Lemanov V V 1999 *Ferroelectrics* **226** 133
[33] Maletic S, Popovic D and Dojcilovic J 2010 *J. Alloys Compd.* **496** 388
[34] Shannon R D 1976 *Acta Cryst. A* **32** 751
[35] Eichel R A 2007 *J. Electroceram.* **19** 11
[36] Tsur Y, Dunbar T D and Randall C A 2001 *J. Electroceram.* **7** 25
[37] Reik H G and Heese D 1967 *J. Phys. Chem. Solids* **28** 581
[38] Shanthi N and Sarma D D 1998 *Phys. Rev. B* **57** 2153
[39] Palik E D 1998 *Handbook of Optical Constants of Solids* (New York: Academic Press) p. 13
[40] Crandles D A, Timusk T, Garrett J D and Greedan J 1994 *Phys. Rev. B* **49** 4299
[41] Guo X G, Chen X S, Sun Y L, Sun L Z, Zhou X H and Lu W 2003 *Phys. Lett. A* **317** 501
[42] Born M and Wolf E 1999 *Principles of Optics*, 7th edn. (Cambridge: Cambridge University Press) p. 40